18 June 2025 14:52:00

Demonstration of Si-doped Al-rich Regrown Al(Ga)N Films on AlN/Sapphire with >10^{15}/cm³ Carrier Concentration using CCS-MOCVD reactor

Swarnav Mukhopadhyay[a)], Parthasarathy Seshadri, Mobinul Haque, Shuwen Xie, Ruixin Bai, Surjava Sanyal, Guangying Wang, Chirag Gupta, Shubhra S. Pasayat

Department of Electrical and Computer Engineering, University of Wisconsin-Madison, Madison, WI, 53706, USA

[a)] Author to whom correspondence should be addressed: swarnav.mukhopadhyay@wisc.edu

Abstract:

Thin Si-doped Al-rich (x_{Al}>0.85) regrown Al(Ga)N layers were deposited on AlN on Sapphire template using metal-organic chemical vapor deposition (MOCVD) techniques. The optimization of the deposition conditions such as temperature (1150 °C), V/III ratio (750), deposition rate (0.7 Å/s), and Si concentration (6×10^{19}/cm^3) resulted in a high charge carrier concentration (> 10^{15} cm^{-3}) in the Si-doped Al-rich Al(Ga)N films. A pulsed deposition condition with pulsed triethylgallium (TEGa) and a continuous flow of trimethylaluminum (TMAl) and ammonia (NH_3) was employed to achieve a controllable Al composition x_{Al}>0.95 and to prevent unintended Ga incorporation in the AlGaN material deposited using the close-coupled showerhead reactor. Also, the effect of unintentional Si incorporation on free charge carrier concentration at the regrowth interface was studied by varying the thickness of the regrown Al(Ga)N layer from 65 nm to <300 nm. A maximum charge carrier concentration of 4.8×10^{16} /cm^3 and 7.5×10^{15} /cm^3 were achieved for $Al_{0.97}Ga_{0.03}N$ and AlN films with thickness <300 nm compared to previously reported n-Al(Ga)N films with thickness ≥400 nm deposited using MOCVD technique.

High-performance power devices with voltage handling capabilities of several kVs are currently in high demand in the power electronics industry. The ultrawide bandgap (UWBG) semiconductors such as Al-rich Al(Ga)N have shown numerous promise for high-voltage operation[1–6]. Similarly, Al(Ga)N-based deep ultra-violet (DUV) emitters, such as light emitting diodes (LEDs) and laser diodes (LDs) are also showing promising performance[7–10]. Enhancing the performance of power and optoelectronic devices requires adequate doping control in Al-rich AlGaN films. The Al-rich AlGaN films with x_{Al} >0.85 suffer from the low conductivity of the film due to higher activation energy of n and p-type dopants, such as Si and Mg, respectively[11–15]. Si-doped Al-rich $Al_xGa_{1-x}N$ (x_{Al} > 0.85) films often exhibit self-compensation and DX center formation, limiting free charge carrier availability in the film[16–18]. It is also reported that the cation vacancy (V_{III}) complex formation with Si (V_{III}-Si), which behaves like an acceptor trap state is also a conductivity limiting factor[11,16]. Additionally, Al(Ga)N deposited via MOCVD contains unintentional carbon impurities, which act as a compensating acceptor (C_N)[11]. Optimized deposition conditions to reduce V_{III}-Si complex formation require deposition at lower temperatures while reducing C_N formation in Al(Ga)N needs higher deposition temperature[19]. So, a trade-off must be created to obtain highly conductive films. Si-doped AlN films (Al-polar and

N-polar) deposited via MBE exhibits high free carrier concentration (>10^{18}/cm³) due to metal-rich growth conditions and low deposition temperatures, reducing V_{III}-Si formation[12,20]. However, using a similar deposition method with MOCVD is challenging. So far, Taniyasu et al.[21,22] and Bagheri et al.[23] have shown ~10^{17}/cm^3 [21] and ~2×10^{15}/cm^3 [22,23] of free charge carrier concentration in Si-doped AlN using MOCVD by controlling the Si doping concentration and managing the point defects, respectively.

While much research exists on Si-doped Al-rich Al(Ga)N deposition using vertical and horizontal MOCVD reactors, few studies focus on using close-coupled showerhead (CCS) reactors[16,24,25]. The CCS reactors are widely accepted for commercially producing III-nitride films and are easily scalable[26]. However, the CCS reactors are known to have issues with unintentional Ga incorporation[26,27], which makes it difficult to obtain a controllable Al composition x_{Al}>0.95 in AlGaN. Since AlN has low n-type conductivity, depositing x_{Al}=0.95-0.97 AlGaN may offer better n-type conductivity while minimizing lattice mismatch with AlN buffer layers or the substrate. Also, AlGaN thin films with Al composition x_{Al}=0.1-0.95 have low thermal conductivity compared to AlN or GaN due to dominant phonon-alloy scattering phenomena[28,29]. The phonon-alloy scattering decreases exponentially as the Al composition becomes x_{Al}>0.95, thus the thermal conductivity of AlGaN enhances rapidly[29]. Using AlGaN films (x_{Al}>0.95) with higher thermal conductivity enhances heat dissipation, benefiting power electronics and deep UV emitters.

In both power electronics and DUV emitters, low-resistive Al-rich n-AlGaN is required to obtain ohmic contacts[30,31]. Also, highly conductive n^{++}-AlGaN layers are necessary to establish ohmic contacts to perform Hall measurements on Al-rich n-AlGaN films. It has been observed that obtaining ohmic contact with the Al-rich (x_{Al}>0.85) AlGaN is non-trivial[32]. For low contact resistivity (<1 μΩ·cm²), a high n-type dopant concentration (>10^{19}/cm³), like Si, is required in the Al-rich n-AlGaN layer. However, increased Si doping concentration can degrade material quality and introduce v-pits and dislocations[33], which is undesirable for power and optoelectronic devices. So, developing a low-resistance Al-rich n^{++}-AlGaN layer with smooth surface morphology is crucial for improving the efficiency of the AlGaN-based devices.

In previous studies, regrown III-nitride materials using MOCVD have shown high unintentional Si incorporation at the regrowth interface[34,35]. This high unintentional Si concentration (>5×10^{19} /cm^3) can behave as deep acceptor levels causing reduced free carrier concentration in Si-doped AlN[21,36]. So, reducing unintentional Si incorporation or its adverse effects would increase free charge carrier concentration in regrown Si-doped thin Al-rich Al(Ga)N films.

This study demonstrated an optimized deposition condition of regrown n-type Si-doped Al-rich Al(Ga)N films on an AlN/sapphire template using a CCS MOCVD reactor to maximize free electron concentration. The impact of deposition conditions on free electron concentration was assessed. Controllable Al composition of x_{Al}>0.95 was non-trivial to achieve in the CCS reactor due to unintentional Ga incorporation. Even after increasing the Al-containing precursor flow while keeping the Ga-containing precursor flow constant, the Al composition did not increase. Thus, for obtaining $Al_{0.97}Ga_{0.03}N$, a pulsed deposition condition was pursued, rather than a continuous deposition condition. Furthermore, an unintentional Si incorporation at the AlN template and regrown n-Al(Ga)N interface affected the electrical performance of the regrown n-Al(Ga)N films. A thicker Al(Ga)N layer (>300 nm) exhibited a higher free charge carrier concentration compared to a thinner layer (<100 nm). The total thickness of the Al(Ga)N layer was kept below 300 nm as obtaining a higher conductivity film with a lower thickness would be cost-effective. Finally, this work showed state-of-the-art free carrier concentration with the thinnest layer of regrown n-AlN on AlN/Sapphire template compared with the reported results from n-AlN deposited on different substrates such as bulk AlN, SiC and Sapphire [21–23,37,38].

Al-rich Al(Ga)N films (65±5 nm) were deposited on AlN/sapphire templates in the CCS MOCVD reactor using triethylgallium (TEGa), trimethylaluminum (TMAl) as group-III precursors and ammonia (NH_3) as group-V precursor. Silane was used as a gaseous precursor for Si doping. First, different deposition conditions such as deposition temperatures (1050 ℃, 1100 ℃, 1150 ℃, and 1210 ℃), V/III ratio (530, 750 and 3000), deposition rate (0.52 Å/s, 0.7 Å/s, and 1 Å/s), and Si concentration (4×10^{19} /cm^3, 6×10^{19} /cm^{3,} and 8×10^{19} /cm^3) were used to find the optimized deposition condition to maximize free carrier concentration of n-AlN (Table 1). The V/III ratio was varied by increasing the NH_3 flow while keeping the TMAl flow constant. To adjust the deposition rate of AlN, the TMAl flow rate was altered while maintaining a constant V/III ratio. Next, the TMAl/TEGa ratio was varied to obtain different Al compositions of $Al_xGa_{1-x}N$ ($0.57\leq x_{Al}\leq1$) (Table 2). An Al composition $x_{Al}>0.95$ was achieved with pulsed deposition, continuously supplying TMAl and NH_3, while pulsing TEGa with a 4-second ON/OFF cycle. H_2 served as the carrier gas for Al(Ga)N deposition. Finally, a thickness series of $Al_xGa_{1-x}N$ (x_{Al} =0.97±0.005) and AlN up to 280 nm was conducted to analyze the impact of unintentional Si incorporation at the interface on free charge carrier concentration.

Table 1. Optimization of maximum charge carrier concentration in Si-doped AlN (65±5 nm)

Experiments	Temperature (℃)	V/III ratio	Deposition Rate (Å/s)	Si (/cm^3)	n_s (/cm^3)
E_{A1}	1050	750	0.7	6×10^{19}	4×10^{13}
	1100				1×10^{14}
	1150				1.5×10^{14}
	1210				N/A
E_{A2}	1150	530	0.7	6×10^{19}	6×10^{13}
		750			1.5×10^{14}
		3000			7×10^{13}
E_{A3}	1150	750	0.52	6×10^{19}	2×10^{13}
			0.7		1.5×10^{14}
			1		1.51×10^{14}
E_{A4}	1150	750	0.7	4×10^{19}	1×10^{14}
				6×10^{19}	1.5×10^{14}
				8×10^{19}	N/A

Table 2. Variation of TMAl/TEGa ratio for obtaining different Al composition

Experiments	Temperature (°C)	V/III ratio	Deposition Rate (Å/s)	Si (/cm^3)	TMA/TEGa ratio	x_{Al}
E_{B1}			0.7		∞	1
E_{B2}			~1		12.69	0.97 (Pulsed)
E_{B3}	1150	750	~1	6×10^{19}	12.69	0.95
E_{B4}			0.92		6.43	0.93
E_{B5}			0.88		2.87	0.86
E_{B6}			1.12		0.64	0.57

The composition of the Al(Ga)N was measured using omega-2theta and reciprocal space mapping (RSM) techniques with the high-resolution X-ray diffraction (XRD) Panalytical Empyrean tool. The surface roughness of the Al(Ga)N films was measured by atomic force microscopy (AFM) using Bruker Icon AFM in tapping mode. The carrier concentration of the n-Al(Ga)N films was measured using mercury CV and Hall measurements using Lake Shore MCS-EMP-4T-V and the Toho HL9980 hall measurement systems. The Si concentration and Al/Ga ratio were measured by the secondary ion mass spectroscopy (SIMS) method using the Cameca SIMS measurement tool.

The Si-doped AlN films deposited at different temperatures showed a prominent trend of how the trade-off between V_{III} and C_N can be obtained in Table 1 (E_{A1}). An increase in the temperature from 1050 °C to 1150 °C, increased the free charge carrier concentration from 4×10^{13}/cm^3 to 1.5×10^{14}/cm^3. We speculate that this 3.75 times increase in the charge concentration may have been related to the reduction of the C_N, which acts as an acceptor-type trap. At lower deposition temperatures, C incorporation becomes very high in MOCVD-deposited III-nitride materials due to the formation of C–group-III bonds[23,39,40]. The presence of the methyl groups in the TMAl was the main reason for the C incorporation. Increasing the temperature promotes the elimination of C from the group-III element by breaking the C–group-III bonds. A sharp decrease in the carrier concentration was observed when the deposition temperature was increased beyond 1150 °C. It was demonstrated previously in the literature that with increasing deposition temperature, the V_{III} formation increases[16,23,40]. So, the probability of V_{III}-Si complex formation increases rapidly. Thus, the sharp decrease in carrier concentration was presumably related to the V_{III}-Si complex formation, like the trend observed by *Washiyama et al*.[23,40]. As the maximum charge was observed at 1150 °C, the rest of the experiments were performed at 1150 °C.

In the next set of experiments, the V/III ratio was varied from 530 to 3000 to identify the effect of C_N and N vacancy formation on the free charge carrier concentration, as shown in Table 1 (E_{A2}). At a low V/III ratio (530), the N vacancy formation probably increased which enhanced the C incorporation in the N sites, forming C_N[40]. It caused a lower charge carrier concentration of 6×10^{13}/cm^3. When the V/III ratio was increased from 530 to 750, the charge increased by 2.5

18 June 2025 14:52:00

times, reaching $1.5\times10^{14}/cm^3$, indicating less C_N formation. However, a high V/III ratio (3000) decreased the charge carrier concentration again from $1.5\times10^{14}/cm^3$ to $7\times10^{13}/cm^3$. We speculate that the reduction in the charge carrier concentration was related to the increased group-III vacancy formation with increased NH_3[40].

Next, the effect of the deposition rate on the charge carrier concentration was observed, shown in Table 1 (E_{A3}). The increase in deposition rate from 0.57 Å/s to 0.72 Å/s showed an increase in the charge concentration from $2\times10^{13}/cm^3$ to $1.5\times10^{14}/cm^3$. We speculate that increased deposition rate reduced desorption of group-III species, suppressing V_{III} formation, similar to findings in high-composition n-AlGaN layers reported by another group in ref. [41]. However, with increasing TMAl flow rate the unintentional C concentration also increases, thus the chances of C_N formation also increase[39,41,42]. So, a very high TMAl flow rate would cause detrimental effects in terms of film conductivity. A further increase in the deposition rate from 0.72 Å/s to 1 Å/s, did not increase the charge carrier concentration significantly, likely due to the trade-off between reduced V_{III} and increased C_N concentration with increasing TMAl flow rate[41]. Further increments in the TMAl flow rate can increase C_N formation. Thus, the deposition rate was maintained at 0.7 Å/s to avoid excess C_N formation.

Next, a silicon concentration variation was performed to identify the optimal Si concentration needed to obtain the highest charge in the AlN layers as shown in Table 1 (E_{A4}). As expected, increasing the Si concentration from $4\times10^{19}/cm^3$ to $6\times10^{19}/cm^3$ increased the charge concentration from 10^{14} $/cm^3$ to 1.5×10^{14} $/cm^3$. However, increasing Si concentration from $6\times10^{19}/cm^3$ to $8\times10^{19}/cm^3$ decreased the charge concentration sharply, indicating the self-compensation phenomena of Si[23,40]. At very high Si concentrations, the V_{III}-Si complex formation, which acts as a compensator, becomes more energetically favorable[40]. Thus, at high Si concentrations, the V_{III}-Si complex concentration increases, enhancing the compensation of free charge carriers and causing Si self-compensation[40]. So, a Si concentration of $6\times10^{19}/cm^3$ was chosen to be optimal.

All n-AlN samples (E_{A1}-E_{A4}) had similar dislocation densities ($4.2\text{-}4.6\times10^8$ /cm²) measured using omega-rocking curve measurement at (0 0 2) and (1 0 2) AlN reflection, making the effect of dislocation densities on free-carrier concentration negligible.

After optimizing deposition conditions for Si-doped AlN, various Al composition AlGaN films were deposited to assess charge incorporation efficiency in different alloys. It was observed that the charge incorporation efficiency exponentially increased with the increase of Ga mole fraction in AlGaN[43]. Nearly 5 orders of magnitude increase in charge carrier concentration was observed when the Ga mole fraction increased from x_{Ga} 0 to 0.43 (Figure 1). Also, the mobility of the Al(Ga)N film increased from ~7 cm^2/Vs to 45 cm^2/Vs with increasing Ga mole fraction (x_{Ga}) from 0 to 0.43. The mobility of the n-$Al_{0.57}Ga_{0.43}N$ film (45 cm^2/Vs) was similar to that reported mobility (30-86 cm^2/Vs) in the literature[41,44–47] for n-AlGaN films (x_{Al}=0.60±0.03) and charge of $10^{18}\text{-}2\times10^{19}/cm^3$. Further mobility improvement is possible by enhancing the material's crystalline quality. Achieving AlGaN with $x_{Ga}<0.05$ in the CCS reactor was non-trivial, as the Ga mole fraction (x_{Ga}) saturated at 0.05. Increasing TMAl flow by 38% did not reduce the Ga mole fraction, with both TMAl and TEGa precursors flowing continuously (continuous deposition mode). This saturation of Ga incorporation was mostly related to the unintentional Ga incorporation in the reactor chamber, as also reported elsewhere[26,27]. So, for obtaining $Al_{0.97}Ga_{0.03}N$, the pulsed deposition condition was used as described in the experimental methods section. The deposition rate of the pulsed and continuous modes was identical due to the TMAl molar flow-dominated deposition condition. Pulsed mode deposition showed no superlattice or forbidden peak (0 0 L, where L is an odd number) in the omega-2theta XRD scan[48,49], confirming uniform Ga incorporation in the AlGaN films.

AFM scans showed that with a reduction of Ga composition, surface roughness increased for Al(Ga)N films (65±5 nm) deposited with continuous deposition mode. However, a clear difference in the surface roughness was observed between the continuous deposition mode and the pulsed deposition mode thin films. The pulsed deposition mode showed almost 4 times lower surface roughness (0.42 nm) compared to all the continuous mode samples (trend line) (Figure 2). We speculate the pulsed mode deposition increased the diffusion length of the group-III adatoms which helped to improve the surface roughness[50].

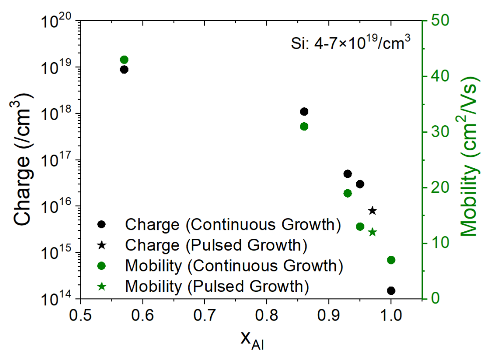

Figure 1. Charge concentration in different Al compositions of Al(Ga)N films (65±5 nm) with a Si concentration between 4-7×10^{19}/cm^3

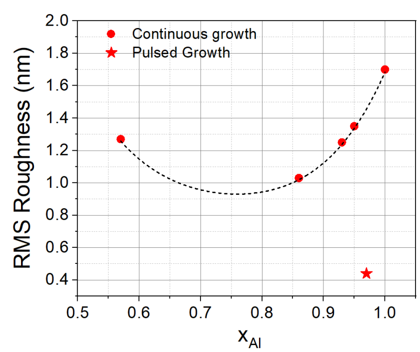

Figure 2. Effect of the surface roughness (AFM scan of 10×10 μm^2) of the Al(Ga)N films (65±5 nm) with different compositions of the Al and different deposition modes

The SIMS measurement of Si-doped AlN showed very high unintentional Si incorporation at the interface between the regrown AlN and the AlN template (Figure 3a). This closely resembled the high unintentional silicon incorporation observed in regrown GaN films using MOCVD, as documented in the literature[34,35]. The unintentional Si incorporation was related to the presence of the residual Si in the MOCVD chamber as reported previously[35]. It was hypothesized that this high unintentional silicon incorporation led to carrier compensation[21,36], and pinning the fermi-level away from the conduction band causing a depletion near the regrowth interface. Therefore, increasing the thickness of the regrown layer minimized the adverse effect of the compensating interface and enhanced the free carrier concentration. This suggests that Si-doping in our regrown Al(Ga)N layers was optimal, with actual doping efficiency exceeding measured values in samples with lower thickness (65±5 nm). The charge concentration increased by ~6 times for $Al_{0.97}Ga_{0.03}N$, with 4 times increase in thickness reaching $4.8\times10^{16}/cm^3$, reaching the highest reported free carrier concentration in x_{Al}=0.97±0.005 n-AlGaN. A slight increase in Ga content (x_{Ga}=0.005) was observed from RSM measurements as n-$Al_{0.97}Ga_{0.03}N$ thickness increased from 70 nm to 280 nm, primarily due to v-pit-assisted unintentional Ga incorporation[51]. Similarly, for AlN, the charge was enhanced by almost 50 times achieving $7.5\times10^{15}/cm^3$ while the thickness was increased by 3 times (Figure 3b). This demonstrates that the compensation effect of the unintentional Si incorporation was more drastic in AlN compared to $Al_{0.97}Ga_{0.03}N$. This may be due to the higher likelihood of forming the DX^{-1} state of the Si and V_{III}-Si complex in n-AlN, which significantly reduces the free electron concentration compared to n-AlGaN[52].

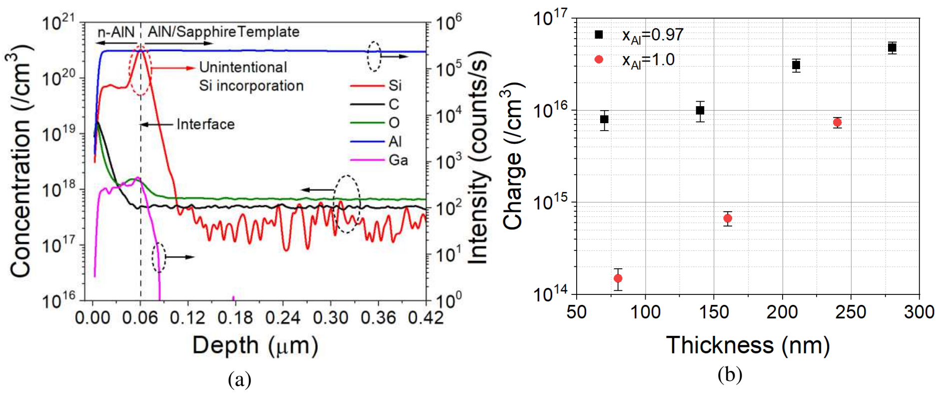

Figure 3. (a) SIMS measurement of Si-doped AlN (65±5nm) film (b) Thickness vs charge concentration for $Al_{0.97}Ga_{0.03}N$ and AlN films

SIMS measurement of Al(Ga)N films (65±5 nm) showed an Al/Ga ratio of ~1000 for AlN, indicating unintentional Ga incorporation (~0.1%) was below the alloy level [53]. Finally, the AFM measurement of 280 nm n-$Al_{0.97}Ga_{0.03}N$ and 240 nm n-AlN showed smooth surface morphology with a surface roughness of 0.56 nm and 0.13 nm (2 µm × 2 µm), respectively (Figure 4). A larger v-pit depth of ~25 nm was observed in n-$Al_{0.97}Ga_{0.03}N$ compared to ~1 nm in n-AlN, which was the reason behind the increased roughness in $Al_{0.97}Ga_{0.03}N$. The v-pit depth difference between n-$Al_{0.97}Ga_{0.03}N$ and n-AlN films with similar Si doping ($6\times10^{19}/cm^3$) may result from ~3 times higher dislocation density and strain in the n-$Al_{0.97}Ga_{0.03}N$ layer. Pulsed deposition conditions will be further improved to reduce dislocation density in the n-$Al_{0.97}Ga_{0.03}N$ layer.

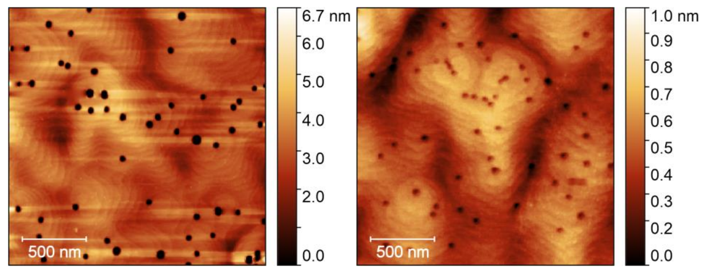

(a) (b)

Figure 4. AFM image (2 μm×2 μm) of (a) 280 nm n-$Al_{0.97}Ga_{0.03}N$ (R_a=0.56 nm) and (b) 240 nm n-AlN (R_a=0.13 nm)

The obtained free charge carrier concentration in Si-doped AlN measured using Hall measurement was compared with the state-of-the-art n-AlN films deposited using MOCVD as reported in the literature (Figure 5). A high free carrier concentration of 7.5×10^{15} /cm^3 with the lowest AlN thickness (240 nm) was demonstrated in this study (Figure 5). This aids n^{++}-AlN contact development for AlN or Al-rich AlGaN power devices and offers insights into improving the regrown interface quality to boost free carrier concentration. However, the mobility was still below 10 cm^2/V.s, which needs to be improved significantly by reducing the dislocation density, as reported previously[23,37].

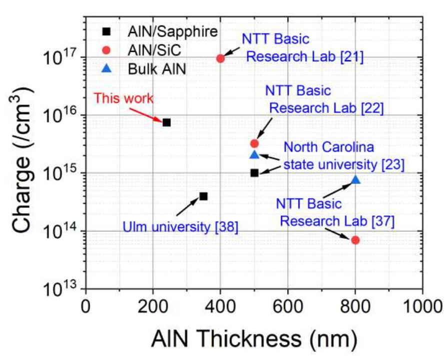

Figure 5. Comparative study of the free charge carrier concentration with AlN thickness for different AlN templates

In conclusion, this study demonstrates methods to obtain high free carrier concentrations in Si-doped high composition (x_{Al}>0.9) AlGaN using a commercially available CCS reactor by optimizing deposition temperature, V/III ratio, deposition rate, and Si concentration. Pulsed deposition yielded $Al_{0.97}Ga_{0.03}N$ in a CCS reactor with 0.42 nm surface roughness and a charge concentration of $4.8\times10^{16}/cm^3$, the highest reported to date. Moreover, the study found that increasing regrown AlN thickness reduces the impact of unintentional Si incorporation at the AlN/sapphire interface, boosting free carrier concentrations. A maximum free carrier concentration of 7.5×10^{15} $/cm^3$ was obtained with 240 nm regrown AlN on the AlN on sapphire templates. Further reduction of DX state formation, Si self-compensation, and V_{III}-Si complex formation would significantly improve charge concentration in n-AlN films, benefiting AlN-based power devices and deep UV emitters.

Acknowledgment:

The authors gratefully acknowledge Lake Shore Cryotronics and Toho Technology for providing the Hall measurement results. The research is partially funded by the NSF CAREER (ECCS-2338683), NSF ASCENT (ECCS-2328137) and ARPA-E ULTRAFAST (AWD00001917).

References:

[1] S. Bajaj, A. Allerman, A. Armstrong, T. Razzak, V. Talesara, W. Sun, S.H. Sohel, Y. Zhang, W. Lu, A.R. Arehart, F. Akyol, and S. Rajan, "High Al-Content AlGaN Transistor With 0.5 A/mm Current Density and Lateral Breakdown Field Exceeding 3.6 MV/cm," IEEE Electron Device Lett. **39**(2), 256–259 (2018).

[2] I. Abid, R. Kabouche, F. Medjdoub, S. Besendorfer, E. Meissner, J. Derluyn, S. Degroote, M. Germain, and H. Miyake, "Remarkable Breakdown Voltage on AlN/AlGaN/AlN double heterostructure," in *2020 32nd International Symposium on Power Semiconductor Devices and ICs (ISPSD)*, (IEEE, Vienna, Austria, 2020), pp. 310–312.

[3] J. Mehta, I. Abid, R. Elwaradi, Y. Cordier, and F. Medjdoub, "Robust $Al_{0.23}Ga_{0.77}N$ channel HFETs on bulk AlN for high voltage power electronics," E-Prime - Advances in Electrical Engineering, Electronics and Energy **5**, 100263 (2023).

[4] D.H. Mudiyanselage, D. Wang, B. Da, Z. He, and H. Fu, "Over 600 V Lateral AlN-on-AlN Schottky Barrier Diodes with Ultra-Low Ideality Factor," Appl. Phys. Express **17**(7), 074001 (2024).

[5] D.H. Mudiyanselage, D. Wang, B. Da, Z. He, and H. Fu, "High-voltage AlN Schottky barrier diodes on bulk AlN substrates by MOCVD," Appl. Phys. Express **17**(1), 014005 (2024).

[6] K. Hussain, A. Mamun, R. Floyd, M.D. Alam, M.E. Liao, K. Huynh, Y. Wang, M. Goorsky, M.V.S. Chandrashekhar, G. Simin, and A. Khan, "High figure of merit extreme bandgap $Al_{0.87}Ga_{0.13}N$-$Al_{0.64}Ga_{0.36}N$ heterostructures over bulk AlN substrates," Appl. Phys. Express **16**(1), 014005 (2023).

[7] B.K. SaifAddin, A.S. Almogbel, C.J. Zollner, F. Wu, B. Bonef, M. Iza, S. Nakamura, S.P. DenBaars, and J.S. Speck, "AlGaN Deep-Ultraviolet Light-Emitting Diodes Grown on SiC Substrates," ACS Photonics **7**(3), 554–561 (2020).

[8] N. Lobo-Ploch, F. Mehnke, L. Sulmoni, H.K. Cho, M. Guttmann, J. Glaab, K. Hilbrich, T. Wernicke, S. Einfeldt, and M. Kneissl, "Milliwatt power 233 nm AlGaN-based deep UV-LEDs on sapphire substrates," Appl. Phys. Lett. **117**(11), (2020).

[9] Z. Zhang, M. Kushimoto, A. Yoshikawa, K. Aoto, C. Sasaoka, L.J. Schowalter, and H. Amano, "Key temperature-dependent characteristics of AlGaN-based UV-C laser diode and demonstration of room-temperature continuous-wave lasing," Appl. Phys. Lett. **121**(22), (2022).

[10] Z. Zhang, M. Kushimoto, M. Horita, N. Sugiyama, L.J. Schowalter, C. Sasaoka, and H. Amano, "Space charge profile study of AlGaN-based p-type distributed polarization doped claddings without impurity doping for UV-C laser diodes," Appl. Phys. Lett. **117**(15), (2020).

[11] I. Bryan, Z. Bryan, S. Washiyama, P. Reddy, B. Gaddy, B. Sarkar, M.H. Breckenridge, Q. Guo, M. Bobea, J. Tweedie, S. Mita, D. Irving, R. Collazo, and Z. Sitar, "Doping and compensation in Al-rich AlGaN grown on single crystal AlN and sapphire by MOCVD," Appl. Phys. Lett. **112**(6), (2018).

[12] H. Ahmad, Z. Engel, C.M. Matthews, S. Lee, and W.A. Doolittle, "Realization of homojunction PN AlN diodes," J. Appl. Phys. **131**(17), (2022).

[13] P. Bagheri, A. Klump, S. Washiyama, M. Hayden Breckenridge, J.H. Kim, Y. Guan, D. Khachariya, C. Quiñones-García, B. Sarkar, S. Rathkanthiwar, P. Reddy, S. Mita, R. Kirste, R. Collazo, and Z. Sitar, "Doping and compensation in heavily Mg doped Al-rich AlGaN films," Appl. Phys. Lett. **120**(8), (2022).

[14] H. Ahmad, J. Lindemuth, Z. Engel, C.M. Matthews, T.M. McCrone, and W.A. Doolittle, "Substantial P-Type Conductivity of AlN Achieved via Beryllium Doping," Advanced Materials **33**(42), 2104497 (2021).

[15] M.E. Zvanut, J.P. Hanle, S. Paudel, R. Page, C. Savant, Y. Cho, H.G. Xing, and D. Jena, "An electron paramagnetic resonance study of the electron transport in heavily Si-doped high Al content AlxGa1−xN," AIP Advances **13**(12), (2023).

[16] I. Prozheev, F. Mehnke, T. Wernicke, M. Kneissl, and F. Tuomisto, "Electrical compensation and cation vacancies in Al rich Si-doped AlGaN," Appl. Phys. Lett. **117**(14), (2020).

[17] M.S. Brandt, R. Zeisel, S.T.B. Gönnenwein, M.W. Bayerl, and M. Stutzmann, "DX behaviour of Si donors in AlGaN alloys," Physica Status Solidi (b) **235**(1), 13–19 (2003).

[18] X.T. Trinh, D. Nilsson, I.G. Ivanov, E. Janzén, A. Kakanakova-Georgieva, and N.T. Son, "Stable and metastable Si negative-U centers in AlGaN and AlN," Appl. Phys. Lett. **105**(16), (2014).

[19] J. Wang, F. Xu, L. Zhang, J. Lang, X. Fang, Z. Zhang, X. Guo, C. Ji, C. Ji, F. Tan, X. Yang, X. Kang, Z. Qin, N. Tang, X. Wang, W. Ge, and B. Shen, "Progress in efficient doping of Al-rich AlGaN," J. Semicond. **45**(2), 021501 (2024).

[20] M.I. Khan, C. Lee, and E. Ahmadi, "Demonstration of controllable Si doping in N-polar AlN using plasma-assisted molecular beam epitaxy," Appl. Phys. Lett. **124**(6), (2024).

[21] Y. Taniyasu, M. Kasu, and N. Kobayashi, "Intentional control of n-type conduction for Si-doped AlN and $Al_XGa_{1-X}N$ ($0.42 \leqslant x < 1$)," Appl. Phys. Lett. **81**(7), 1255–1257 (2002).

[22] Y. Taniyasu, M. Kasu, and T. Makimoto, "Electrical conduction properties of n-type Si-doped AlN with high electron mobility ($>100 cm^2V^{-1}s^{-1}$)," Appl. Phys. Lett. **85**(20), 4672–4674 (2004).

[23] P. Bagheri, C. Quiñones-Garcia, D. Khachariya, S. Rathkanthiwar, P. Reddy, R. Kirste, S. Mita, J. Tweedie, R. Collazo, and Z. Sitar, "High electron mobility in AlN:Si by point and extended defect management," J. Appl. Phys. **132**(18), (2022).

[24] J. Stellmach, M. Pristovsek, Ö. Savaş, J. Schlegel, E.V. Yakovlev, and M. Kneissl, "High aluminium content and high growth rates of AlGaN in a close-coupled showerhead MOVPE reactor," Journal of Crystal Growth **315**(1), 229–232 (2011).

[25] L. Spasevski, G. Kusch, P. Pampili, V.Z. Zubialevich, D.V. Dinh, J. Bruckbauer, P.R. Edwards, P.J. Parbrook, and R.W. Martin, "A systematic comparison of polar and semipolar Si-doped AlGaN alloys with high AlN content," J. Phys. D: Appl. Phys. **54**(3), 035302 (2020).

[26] G. Deng, L. Zhang, Y. Wang, J. Yu, Y. Niu, H. Qian, X. Li, Z. Shi, and Y. Zhang, "Ga-free AlInN films growth by close-coupled showerhead metalorganic chemical vapor deposition," Micro and Nanostructures **165**, 207191 (2022).

[27] M. Mrad, Y. Mazel, G. Feuillet, and M. Charles, "Avoiding Gallium Pollution in Close-Coupled Showerhead Reactors, Alternative Process Routes," Physica Status Solidi (a) **220**(16), 2200824 (2023).

[28] W. Liu, and A.A. Balandin, "Thermal conduction in AlxGa1−xN alloys and thin films," J. Appl. Phys. **97**(7), (2005).

[29] D.Q. Tran, R.D. Carrascon, M. Iwaya, B. Monemar, V. Darakchieva, and P.P. Paskov, "Thermal conductivity of $Al_xGa_{1-x}N$ (0<=x<=1) epitaxial layers," Phys. Rev. Mater. **6**(10), 104602 (2022).

[30] M. Hiroki, Y. Taniyasu, and K. Kumakura, "High-Temperature Performance of AlN MESFETs With Epitaxially Grown n-Type AlN Channel Layers," IEEE Electron Device Lett. **43**(3), 350–353 (2022).

[31] M. Kneissl, T.-Y. Seong, J. Han, and H. Amano, "The emergence and prospects of deep-ultraviolet light-emitting diode technologies," Nat. Photonics **13**(4), 233–244 (2019).

[32] R. France, T. Xu, P. Chen, R. Chandrasekaran, and T.D. Moustakas, "Vanadium-based Ohmic contacts to n-AlGaN in the entire alloy composition," Appl. Phys. Lett. **90**(6), (2007).
[33] D. Nilsson, E. Janzén, and A. Kakanakova-Georgieva, "Strain and morphology compliance during the intentional doping of high-Al-content AlGaN layers," Appl. Phys. Lett. **105**(8), (2014).
[34] K. Fu, H. Fu, X. Deng, P.-Y. Su, H. Liu, K. Hatch, C.-Y. Cheng, D. Messina, R.V. Meidanshahi, P. Peri, C. Yang, T.-H. Yang, J. Montes, J. Zhou, X. Qi, S.M. Goodnick, F.A. Ponce, D.J. Smith, R. Nemanich, and Y. Zhao, "The impact of interfacial Si contamination on GaN-on-GaN regrowth for high power vertical devices," Appl. Phys. Lett. **118**(22), (2021).
[35] M. Noshin, R. Soman, X. Xu, and S. Chowdhury, "A systematic study of the regrown interface impurities in unintentionally doped Ga-polar c-plane GaN and methods to reduce the same," Semicond. Sci. Technol. **37**(7), 075018 (2022).
[36] F. Mehnke, X.T. Trinh, H. Pingel, T. Wernicke, E. Janzén, N.T. Son, and M. Kneissl, "Electronic properties of Si-doped $Al_xGa_{1-x}N$ with aluminum mole fractions above 80%," J. Appl. Phys. **120**(14), (2016).
[37] Y. Taniyasu, M. Kasu, and T. Makimoto, "Increased electron mobility in n-type Si-doped AlN by reducing dislocation density," Appl. Phys. Lett. **89**(18), (2006).
[38] S.B. Thapa, J. Hertkorn, F. Scholz, G.M. Prinz, R.A.R. Leute, M. Feneberg, K. Thonke, R. Sauer, O. Klein, J. Biskupek, and U. Kaiser, "Growth and studies of Si-doped AlN layers," Journal of Crystal Growth **310**(23), 4939–4941 (2008).
[39] A.S. Almogbel, C.J. Zollner, B.K. Saifaddin, M. Iza, J. Wang, Y. Yao, M. Wang, H. Foronda, I. Prozheev, F. Tuomisto, A. Albadri, S. Nakamura, S.P. DenBaars, and J.S. Speck, "Growth of highly conductive Al-rich AlGaN:Si with low group-III vacancy concentration," AIP Advances **11**(9), (2021).
[40] S. Washiyama, P. Reddy, B. Sarkar, M.H. Breckenridge, Q. Guo, P. Bagheri, A. Klump, R. Kirste, J. Tweedie, S. Mita, Z. Sitar, and R. Collazo, "The role of chemical potential in compensation control in Si:AlGaN," J. Appl. Phys. **127**(10), (2020).
[41] J. Yang, Y.H. Zhang, D.G. Zhao, P. Chen, Z.S. Liu, and F. Liang, "Realization low resistivity of high AlN mole fraction Si-doped AlGaN by suppressing the formation native vacancies," Journal of Crystal Growth **570**, 126245 (2021).
[42] D.D. Koleske, A.E. Wickenden, R.L. Henry, and M.E. Twigg, "Influence of MOVPE growth conditions on carbon and silicon concentrations in GaN," Journal of Crystal Growth **242**(1–2), 55–69 (2002).
[43] F. Mehnke, T. Wernicke, H. Pingel, C. Kuhn, C. Reich, V. Kueller, A. Knauer, M. Lapeyrade, M. Weyers, and M. Kneissl, "Highly conductive n-$Al_xGa_{1-x}N$ layers with aluminum mole fractions above 80%," Appl. Phys. Lett. **103**(21), (2013).
[44] K. Kataoka, T. Narita, Y. Yagi, K. Nagata, and Y. Saito, "Comprehensive Study of Electron Conduction and Its Compensation for Degenerate Si-Doped AlN-Rich AlGaN," Physica Status Solidi (RRL) – Rapid Research Letters **18**(2), 2300055 (2024).
[45] K.B. Nam, J. Li, M.L. Nakarmi, J.Y. Lin, and H.X. Jiang, "Achieving highly conductive AlGaN alloys with high Al contents," Appl. Phys. Lett. **81**(6), 1038–1040 (2002).
[46] P. Pampili, D.V. Dinh, V.Z. Zubialevich, and P.J. Parbrook, "Significant contribution from impurity-band transport to the room temperature conductivity of silicon-doped AlGaN," J. Phys. D: Appl. Phys. **51**(6), 06LT01 (2018).
[47] K. Nagata, H. Makino, T. Yamamoto, K. Kataoka, T. Narita, and Y. Saito, "Low resistivity of highly Si-doped n-type Al0.62Ga0.38N layer by suppressing self-compensation," Appl. Phys. Express **13**(2), 025504 (2020).
[48] D. Korakakis, K.F. Ludwig, and T.D. Moustakas, "Long range order in $Al_xGa_{1-x}N$ films grown by molecular beam epitaxy," Appl. Phys. Lett. **71**(1), 72–74 (1997).
[49] W.H. Sun, J.P. Zhang, J.W. Yang, H.P. Maruska, M.A. Khan, R. Liu, and F.A. Ponce, "Fine structure of AlN/AlGaN superlattice grown by pulsed atomic-layer epitaxy for dislocation filtering," Appl. Phys. Lett. **87**(21), (2005).

[50] I. Ahmad, B. Krishnan, B. Zhang, Q. Fareed, M. Lachab, J. Dion, and A. Khan, "Dislocation reduction in high Al-content AlGaN films for deep ultraviolet light emitting diodes," Physica Status Solidi (a) **208**(7), 1501–1503 (2011).
[51] A. Mogilatenko, J. Enslin, A. Knauer, F. Mehnke, K. Bellmann, T. Wernicke, M. Weyers, and M. Kneissl, "V-pit to truncated pyramid transition in AlGaN-based heterostructures," Semicond. Sci. Technol. **30**(11), 114010 (2015).
[52] T.A. Henry, A. Armstrong, A.A. Allerman, and M.H. Crawford, "The influence of Al composition on point defect incorporation in AlGaN," Appl. Phys. Lett. **100**(4), (2012).
[53] M.I. Khan, C. Lee, and E. Ahmadi, "Demonstration of controllable Si doping in N-polar AlN using plasma-assisted molecular beam epitaxy," Appl. Phys. Lett. **124**(6), (2024).